esipap
European School of Instrumentation in Particle & Astroparticle Physics

esi
European Scientific Institute

DETECTOR TECHNOLOGIES

Lecture 3 : Radiation Detectors

- Scintillation
- Čerenkov
- TRD

Jean-Marie Brom (IPHC) – brom@in2p3.fr

Scintillator : a material which emits light (photons), when stimulated

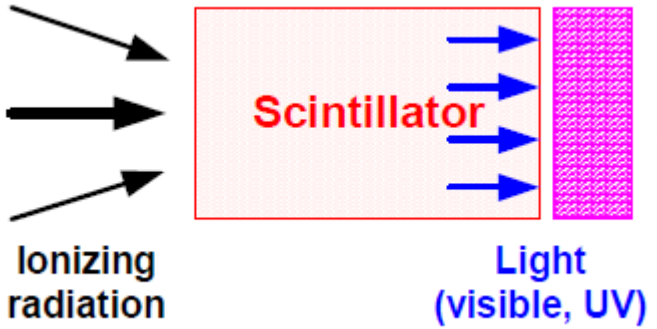

Of course, we need a light sensor to transform the light in an electric signal

Light intensity : $L(t) = Lo\ e^{-\frac{t}{\tau}}$

$\tau \approx$ nsec. - µsec. **Fluorescence**

$\tau \approx$ µsec. - mins **Phosphorescence**

Scintillator

Ligth guide

Photo detector

Read out

For a scintillator, what is important ?

- **Scintillation efficiency** : energy needed for 1 γ - emission
- **Light spectrum** : in order to adapt the read out system to the proper wavelength
- **Light decay time**
- **γ absorption**
- **Transparency** : the emitted γ should not be re-absorbed.

2 types of scintillators :

Organics (liquids, plastics)

Advantage : Fast

Disadvantages : rather innefficients

non-linear (need quenching)

not good for γ 's

Used mainly for trigger purpose

Inorganics (crystals,liquids)

Advantages : good efficiency

good linearity

radiation tolerance

Disadvantages : relatively slow

expensive (if crystals)

Used mainly for measurements

Organic Scintillators :

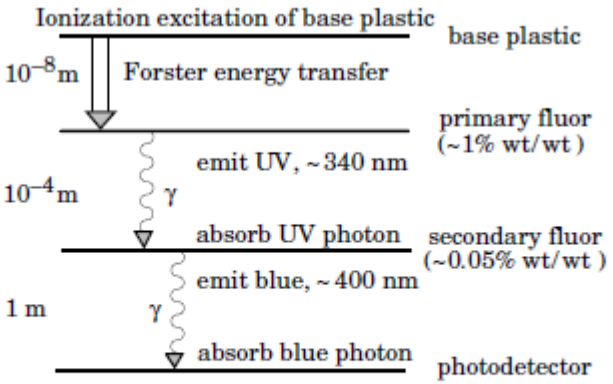

Figure 28.1: Cartoon of scintillation "ladder" depicting the operating mechanism of organic scintillator. Approximate fluor concentrations and energy transfer distances for the separate sub-processes are shown.

1. Excitation of organic molecules
   Yield ≈ 1 γ per loss of 100 eV
   γ λ ≈100 nm (UV)
1. Absorption and re-emission
   γ λ ≈300 nm (UV)
2. Absorption and re-emission
   γ λ ≈ 400 nm (Blue)

Wave shifter (adapts to the read-out)
slows the process
induce a non-linearity

Luminescence (Birk's law) per lenght

$$\frac{dL}{dx} = \frac{S\,\frac{dE}{dx}}{1 + KB\,\frac{dE}{dx}}$$

S = emission efficiency
KB = Birk's constant (exp.)

Low Z (organic = Hydrogen + Carbon)
low efficiency for HE γ (only Compton effect)
but good efficiency for neutrons

Scintillation : Organic scintillators

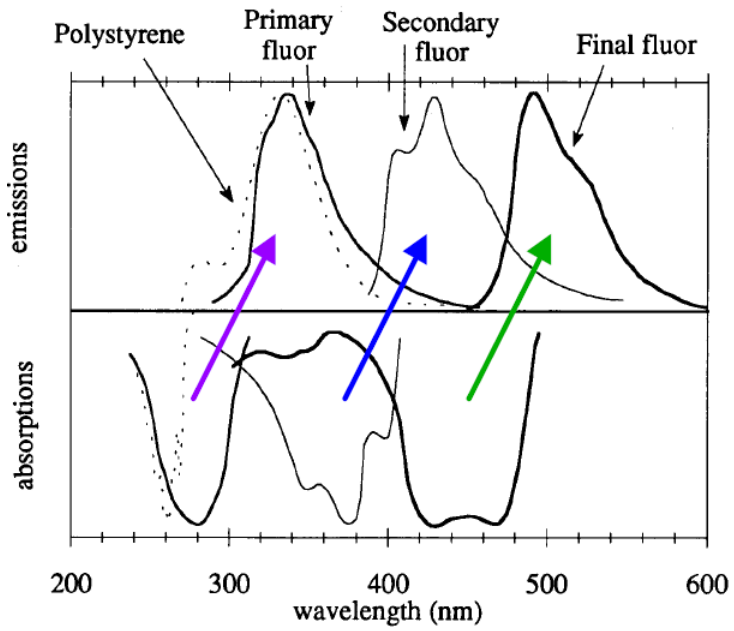

Wavelenght shift

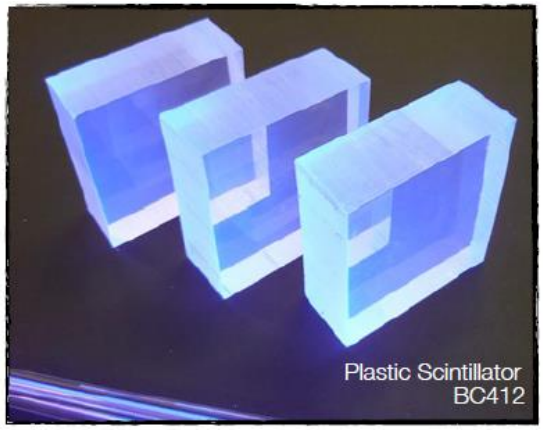

Table A6.3 Properties of some organic scintillators

scintillator	density (g/cm^3)	index of refraction	wavelength of maximum emission (nm)	decay time constant (ns)	scintillation pulse height [1]	H/C ratio [2]
Monocrystals						
naphthalene	1.15	1.58	348	11	11	0.800
anthracene	1.25	1.59	448	30-32	100	0.714
trans-stilbene	1.16	1.58	384	3-8	46	0.857
p-terphenyl	1.23		391	6-12	30	0.778
Plastics [3]						
NE 102 A	1.032	1.58	425	2.5	65	1.105
NE 104	1.032	1.58	405	1.8	68	1.100
NE 110	1.032	1.58	437	3.3	60	1.105
NE 111	1.032	1.58	370	1.7	55	1.096
Plastics [4]						
BC-400	1.032	1.581	423	2.4	65	1.103
BC-404	1.032	1.58	408	1.8	68	1.107
BC-408	1.032	1.58	425	2.1	64	1.104
BC-412	1.032	1.58	434	3.3	60	1.104
BC-414	1.032	1.58	392	1.8	68	1.110
BC-416	1.032	1.58	434	4.0	50	1.110
BC-418	1.032	1.58	391	1.4	67	1.100
BC-420	1.032	1.58	391	1.5	64	1.100
BC-422	1.032	1.58	370	1.6	55	1.102
BC-422Q	1.032	1.58	370	0.7	11	1.102
BC-428	1.032	1.58	480	12.5	50	1.103
BC-430	1.032	1.58	580	16.8	45	1.108
BC-434	1.049	1.58	425	2.2	60	0.995

Crystals (NaI, CsI, BGO, PbWO4…)

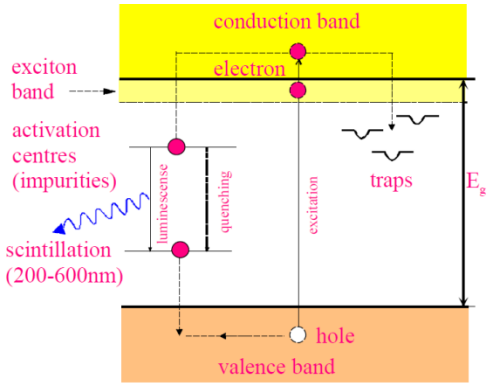

Energy loss will induce electron-hole pairs creation
migration to activation centers (fast)
- excitation – transition - γ emission
trapping (slow)

Activator is choosen for visible emission
2 or more wavelenghts (addition of activator)

Liquid noble gases (Lar, Lxe, LKr)

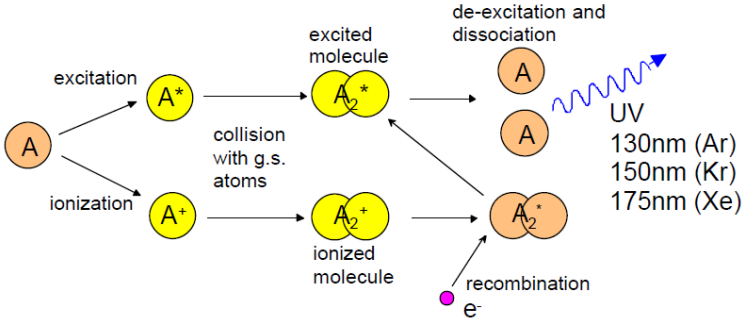

Still 2 time constants
Same wavelengths (pure gases)

Precision measurements

Scintillation : Inorganic scintillators

Table A6.2 Properties of some inorganic scintillators

scintillator composition	density (g/cm^3)	index of refraction	wavelength of maximum emission (nm)	decay time constant (μs)	scintillation pulse height[1]	notes	Photons/ MeV
NaI	3.67	1.78	303	0.06	190	2)	
NaI(Tl)	3.67	1.85	410	0.25	100	3)	4×10^4
CsI	4.51	1.80	310	0.01	6	3)	
CsI(Tl)	4.51	1.80	565	1.0	45	3)	1.1×10^4
CaI(Na)	4.51	1.84	420	0.63	85	3)	
KI(Tl)	3.13	1.71	410	0.24/2.5	24	3)	
^{6}LiI(Eu)	4.06	1.96	470-485	1.4	35	3)	1.4×10^4
CaF_2(Eu)	3.19	1.44	435	0.9	50		
BaF_2	4.88	1.49	190/220 310	0.0006 0.63	5 15		6.5×10^3 2×10^3
$Bi_4Ge_3O_{12}$	7.13	2.15	480	0.30	10		2.8×10^3
$CaWO_4$	6.12	1.92	430	0.5/20	50		
$ZnWO_4$	7.87	2.2	480	5.0	26		
$CdWO_4$	7.90	2.3	540	5.0	40		
CsF	4.65	1.48	390	0.005	5	3)	
CeF_3	6.16	1.68	300 340	0.005 0.020	5		
ZnS(Ag)	4.09	2.35	450	0.2	150	4)	
GSO	6.71	1.9	440	0.060	20		
ZnO(Ga)	5.61	2.02	385	0.0004	40	4)	
YSO	4.45	1.8	420	0.035	50		
YAP	5.50	1.9	370	0.030	40		

[1] relative to NaI(Tl) [2] at 80 K [3] hygroscopic [4]polycrystalline

$PbWO_4$	8.28	1.82	440, 530	0.01			100

LAr	1.4	1.29[5]	120-170	0.005 / 0.860			
LKr	2.41	1.40[5]	120-170	0.002 / 0.085			
LXe	3.06	1.60[5]	120-170	0.003 / 0.022			4×10^4

[5] at 170 nm

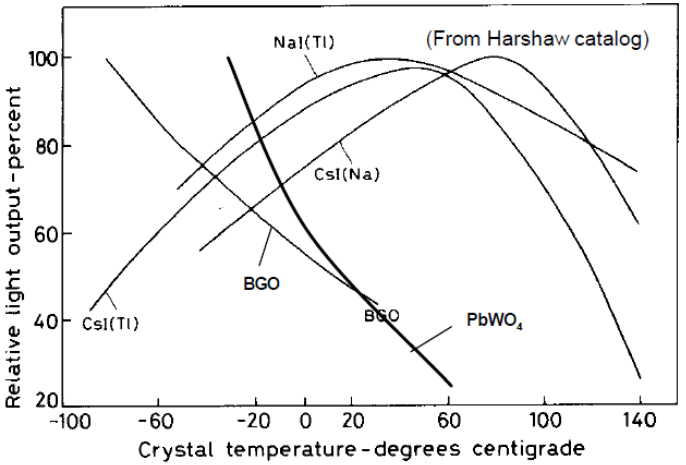

Inorganic crystals are temperature-sensitive (calorimeters have to be cooled)

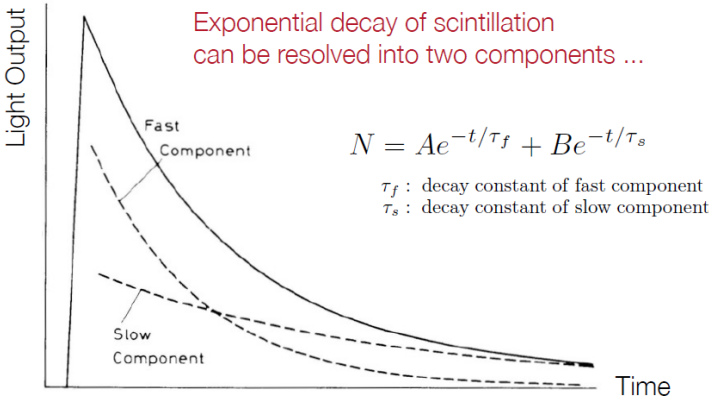

Scintillation : Inorganic scintillators

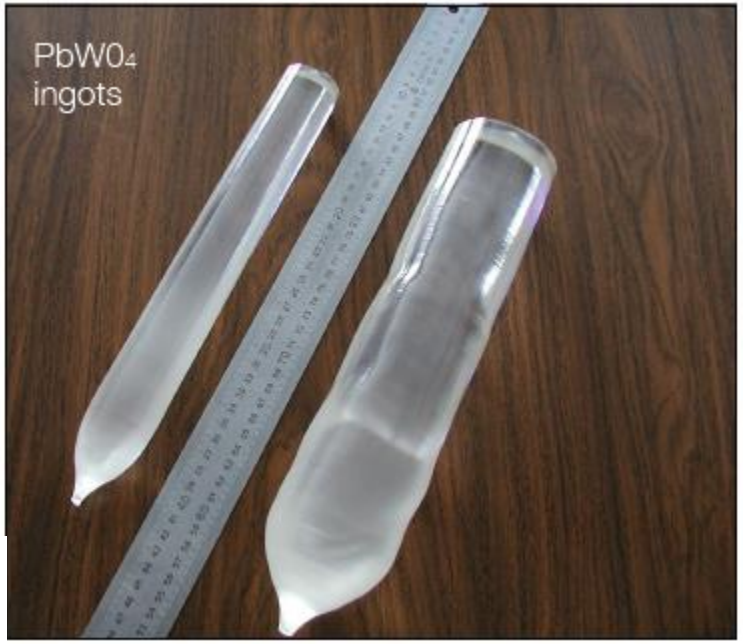

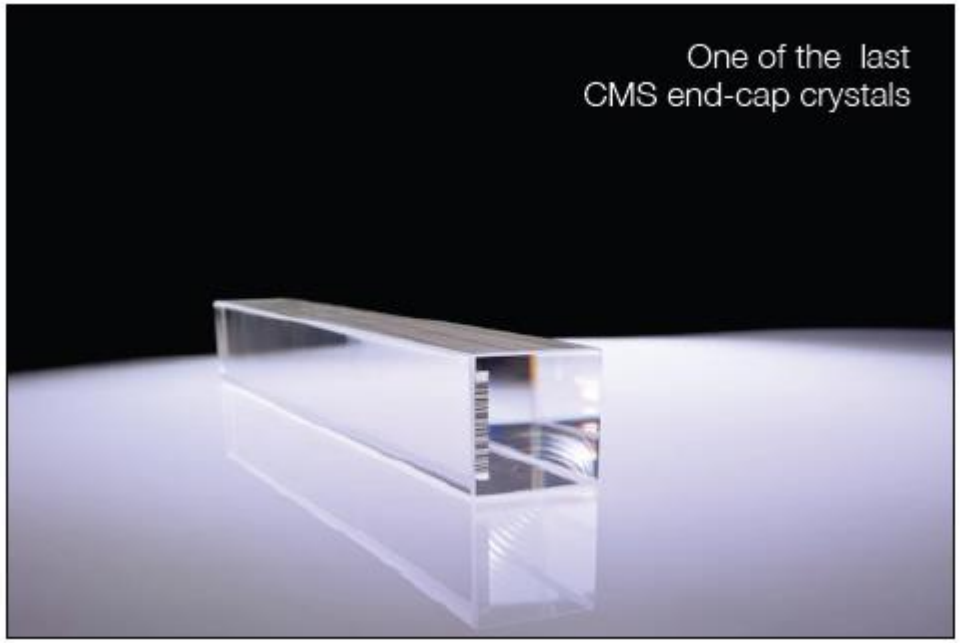

The readout has to be adapted to geometry and emission spectrum of the scintillator.

Light guide

Total reflection inside the light guide

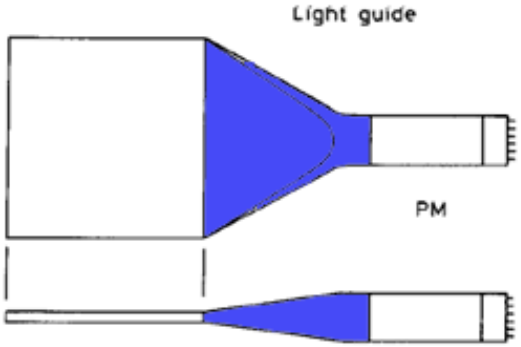

“fish tail”

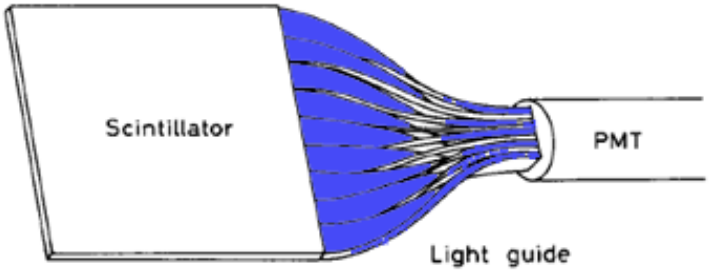

adiabatic

Material :
PPMA (Polymethylmethacrylat)
Plexiglas $(C_5O_2H_8)_n$

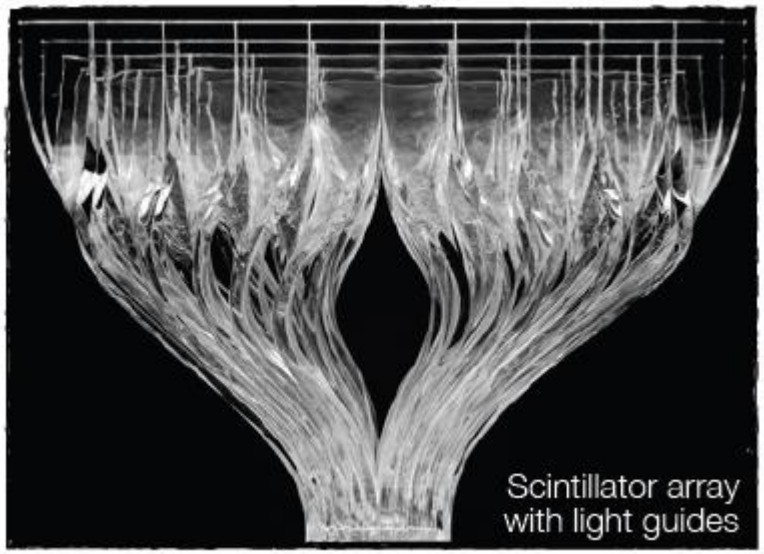

Optical fiber

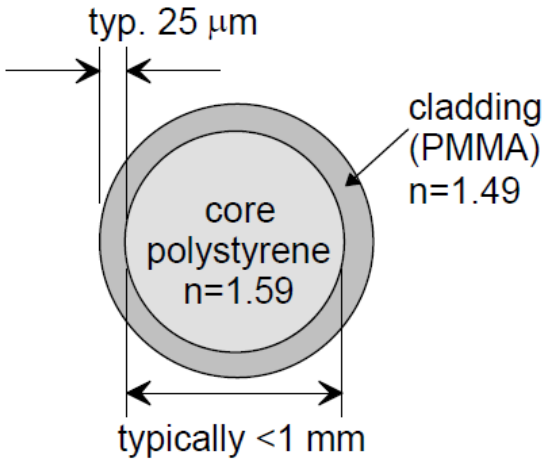

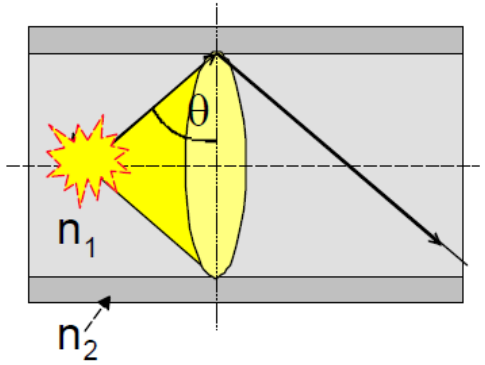

$$\mathrm{NA} = \sqrt{n_{\mathrm{core}}^2 - n_{\mathrm{clad}}^2}$$

$$\theta \geq \arcsin \frac{n_2}{n_1} \approx 69.6^\circ$$

$$\frac{d\Omega}{4\pi} = 3.1\% \quad \text{in one direction}$$

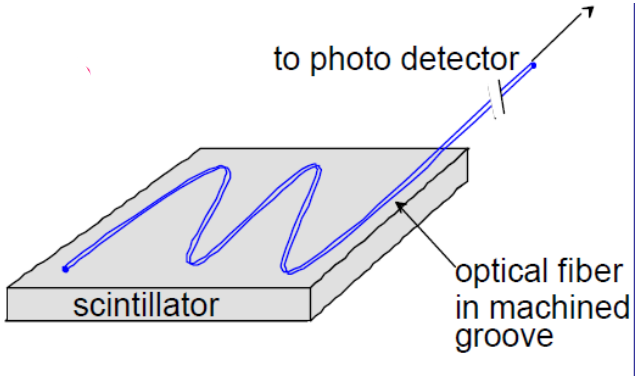

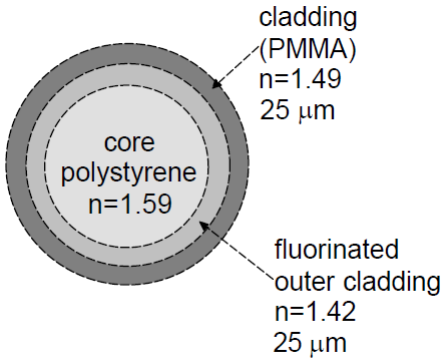

Improved aperture with multi-cladding $\frac{d\Omega}{4\pi} = 5.3\%$

Scintillating fiber : optical fiber filled with scintillator (plastic or liquid)

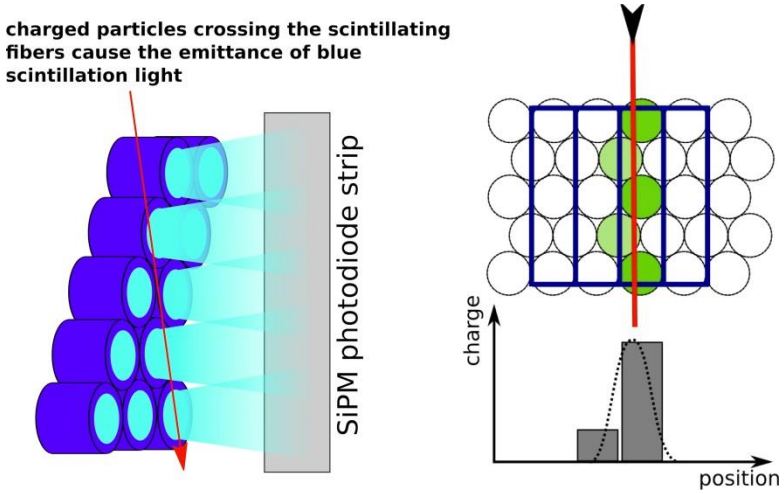

Fiber	Emission Color	Emission Peak, nm	Decay Time, ns	1/e Length m*	# of Photons per MeV**	Characteristics/ Applications
BCF-10	blue	432	2.7	2.2	~8000	General purpose; optimized for diameters >250µm
BCF-12	blue	435	3.2	2.7	~8000	Improved transmission for use in long lengths
BCF-20	green	492	2.7	>3.5	~8000	Fast green scintillator
BCF-60	green	530	7	3.5	~7100	3HF formulation for radiation hardness
BCF-91A	green	494	12	>3.5	n/a	Shifts blue to green
BCF-92	green	492	2.7	>3.5	n/a	Fast blue to green shifter
BCF-98	n/a	n/a	n/a	n/a	n/a	Clear waveguide

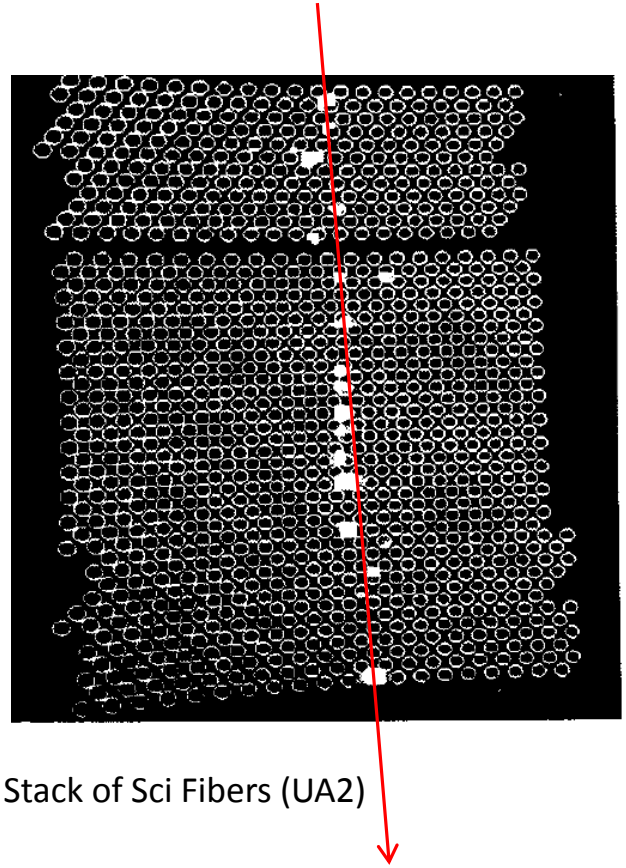

Stack of Sci Fibers (UA2)

Photodetector : Convert the scintillating ligth into usable electronic signal
(HE Physics : usually visible and UV spectrum)
= Convert UV and visible photons in electrons

Requirement : High conversion efficiency QE = $N_{\text{photo-electrons}} / N_{\text{photons}}$

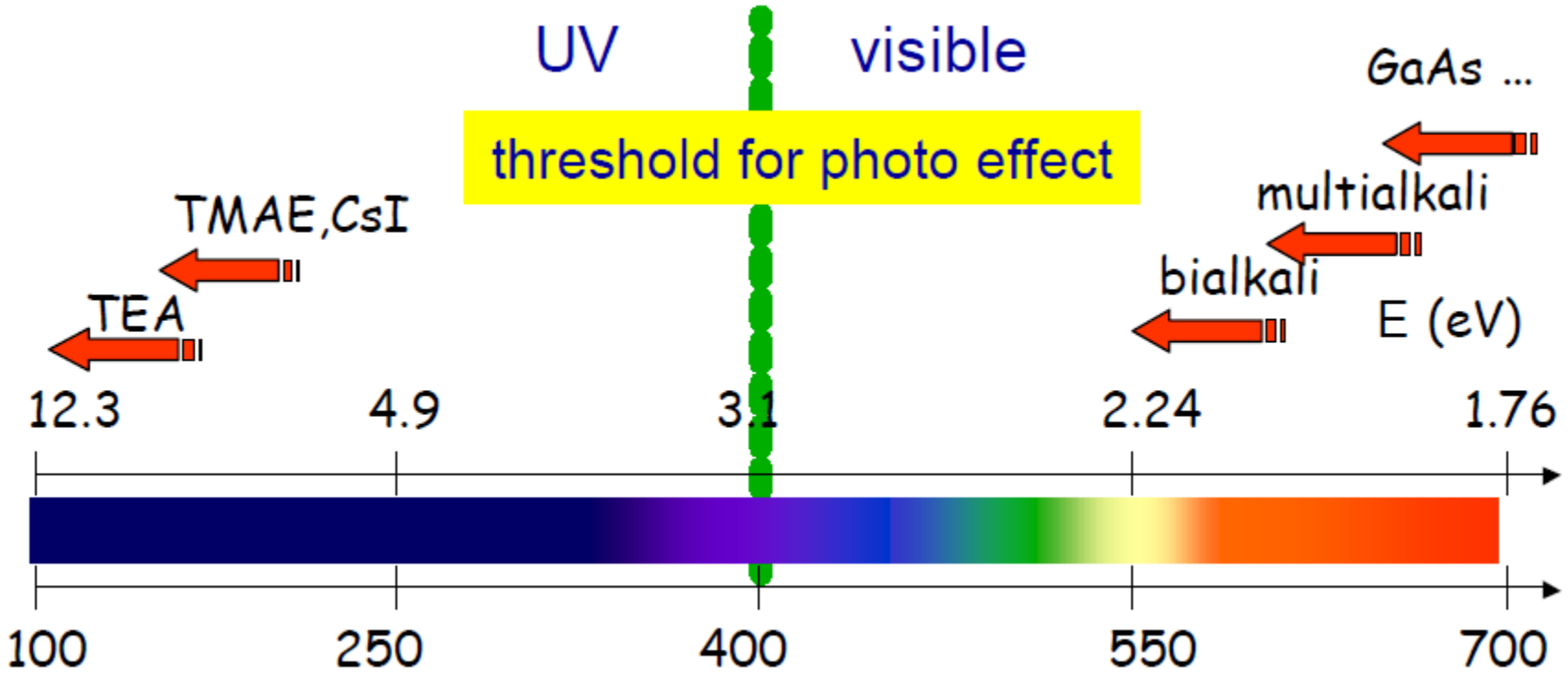

Scintillation : Photomultiplier

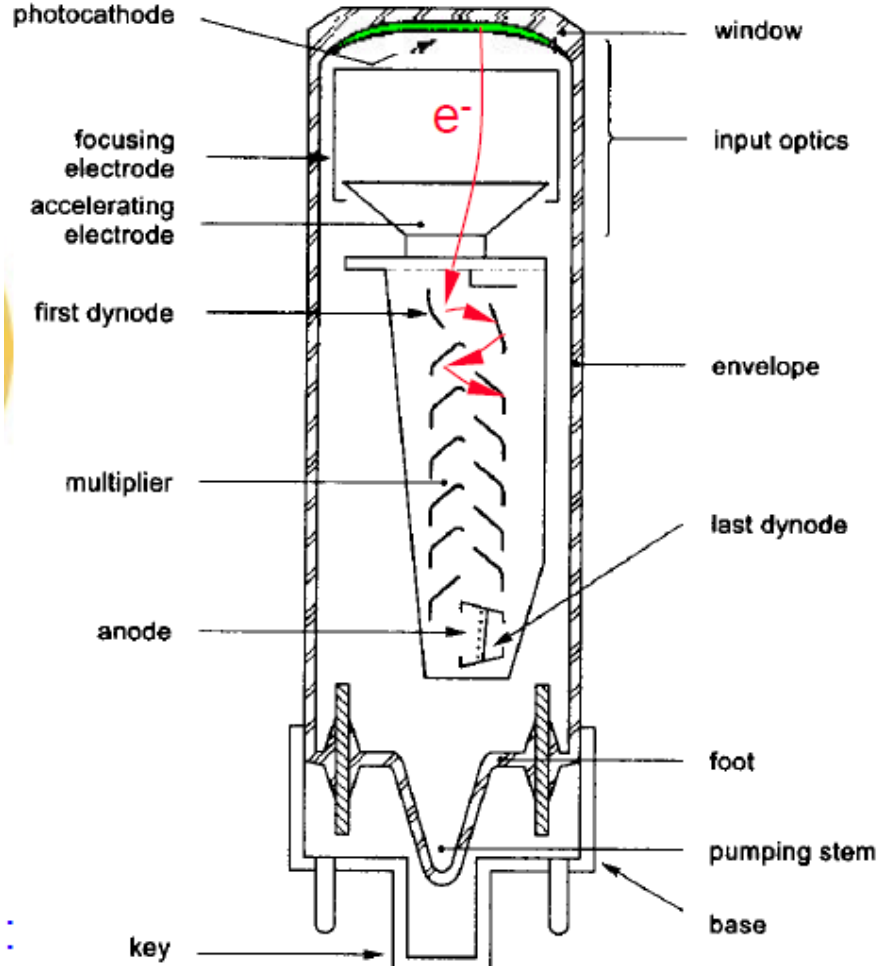

Principle:

Electron emission
from photo cathode

Secondary emission
from dynodes; dynode gain: 3-50 [f(E)]

Typical PMT Gain: > 10^6
[PMT can see single photons ...]

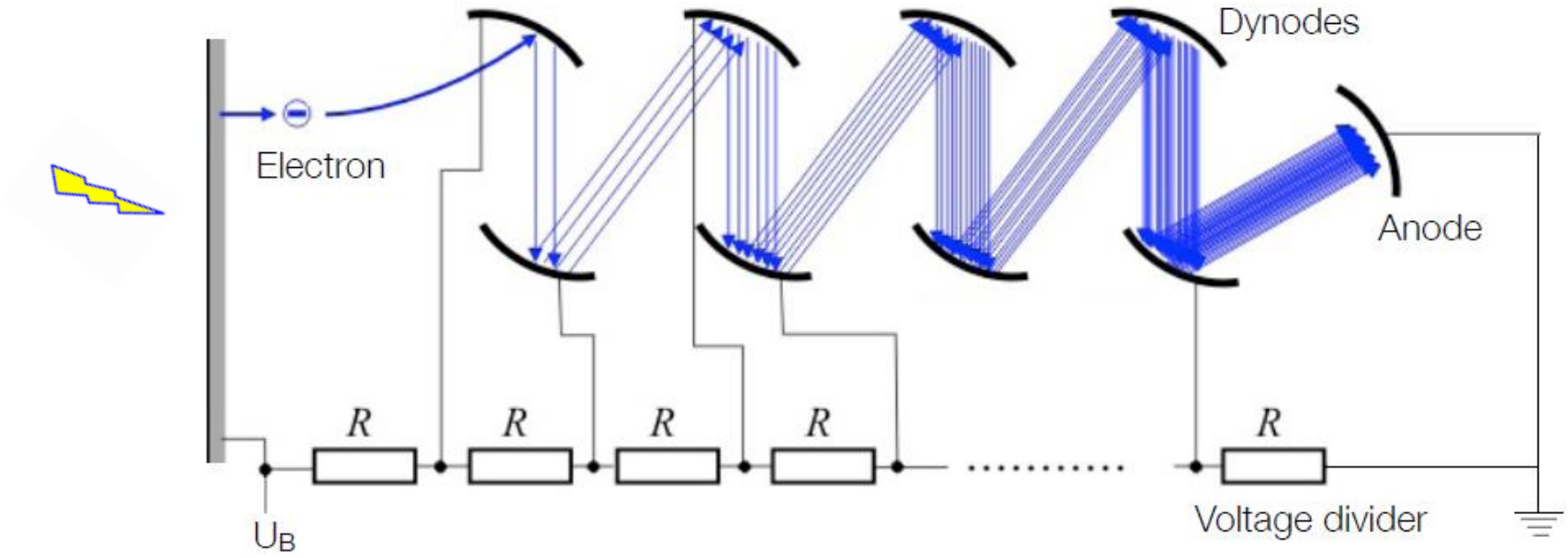

Requirement : High conversion efficiency QE = N $_{\text{photo-electrons}}$ / N $_{\text{photons}}$

Total gain :

Typical: $\delta = 2 - 10$, $n = 8 - 15$] → $G = \delta^n = 10^6 - 10^8$

Resolution : linearity
statistics

δ = N $_{\text{electrons produced}}$ / N $_{\text{electrons incoming}}$
n = number of dynodes

And … Sensitivity to magnetic field

Scintillation : Photomultiplier

Type	Head-on type
Tube Size	Dia.13 mm
Photocathode Area Shape	Round
Photocathode Area Size	Dia.10 mm
Wavelength (Short)	185 nm
Wavelength (Long)	650 nm
Wavelength (Peak)	420 nm
Spectral Response Curve Code	400U
Photocathode Material	Bialkali
Window Material	UV glass
Dynode Structure	Linear-focused
Dynode Stages	10
[Max. Rating] Anode to Cathode Voltage	1250 V
[Max. Rating] Average Anode Current	0.1 mA
Anode to Cathode Supply Voltage	1000 V
[Cathode] Luminous Sensitivity Min.	40 µA/lm
[Cathode] Luminous Sensitivity Typ.	110 µA/lm
[Cathode] Blue Sensitivity Index (CS 5-58) Typ.	10
[Cathode] Radiant Sensitivity Typ.	80 mA/W
[Anode] Luminous Sensitivity Min.	30 A/lm
[Anode] Luminous Sensitivity Typ.	110 A/lm
[Anode] Radiant Sensitivity Typ.	8.0×10^4 A/W
[Anode] Gain Typ.	1.0×10^6
[Anode] Dark Current (after 30min.) Typ.	1 nA
[Anode] Dark Current (after 30min.) Max.	15 nA
[Time Response] Rise Time Typ.	2.1 ns
[Time Response] Transit Time Typ.	22 ns

Multi anode PMT

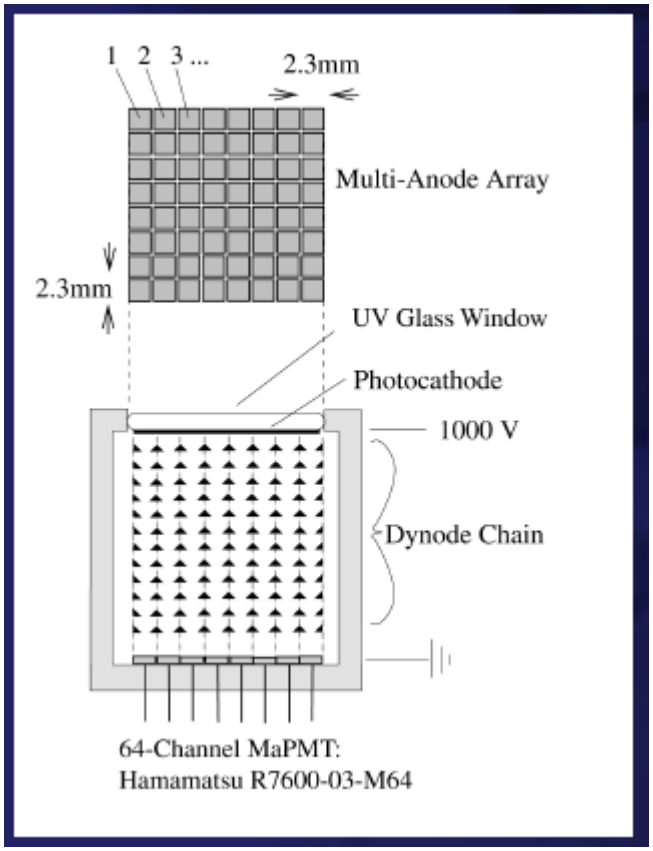

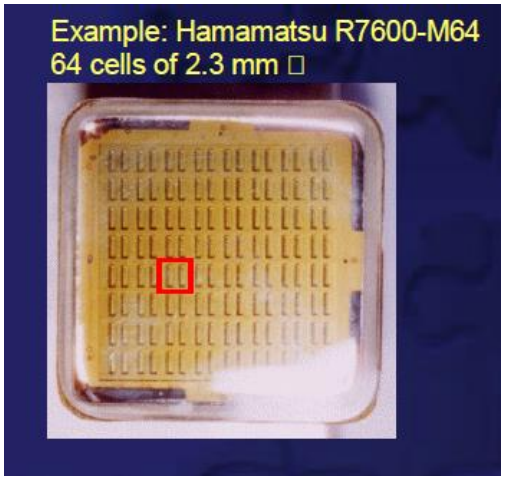

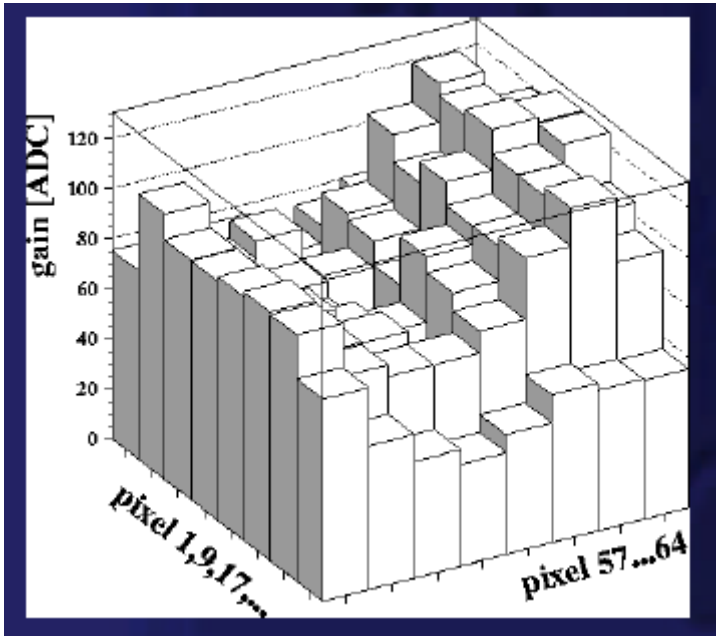

Resistant to magnetic field

Hybrid Photo Diode (HPD) highly segmented read out

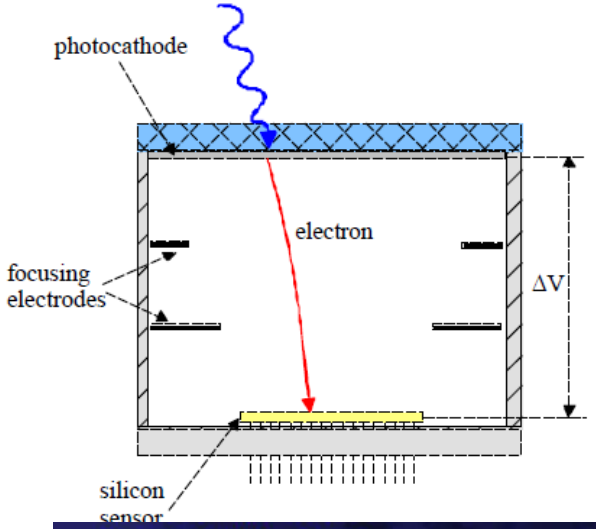

$$G = \frac{e\Delta V}{W_{Si}} = \frac{20\ keV}{3.6\ eV} \approx 5 \cdot 10^3 \quad \text{(for } \Delta V = 20\ \text{kV)}$$

photo cathode + p.e. acceleration + silicon det. (pixel, strip, pads)

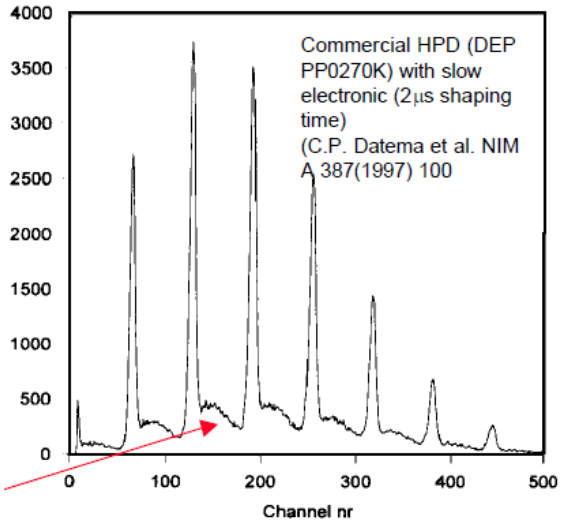

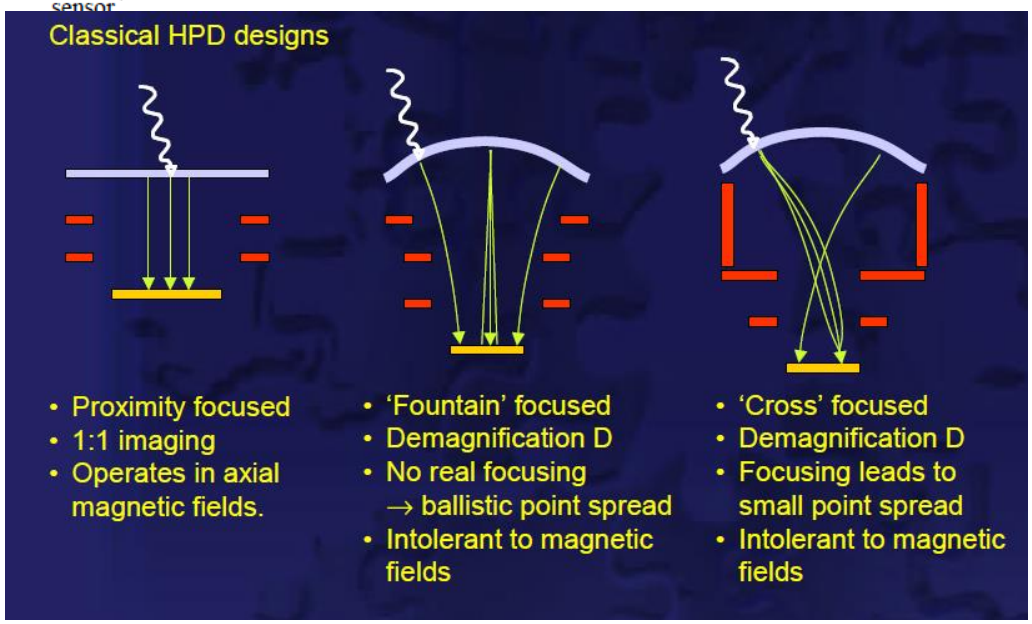

Good sensitivity (PMT like)
Speed
Less sensistive to Mag. Field
Precision

LHCb : Cerenkovs read-out with HPDS

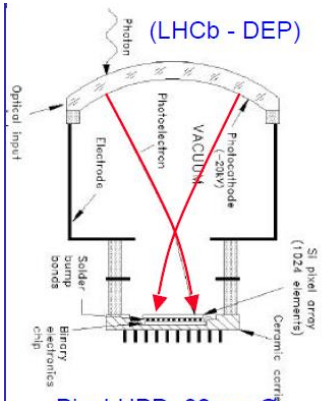

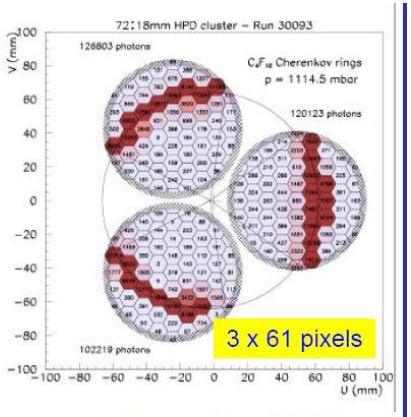

- 484 HPDs (Hybrid Photon Detector) :
  196 for RICH1 and 288 for RICH2
- ~3.3 m² total surface
- Granularity: 2.5 x 2.5 mm²
  (almost 0.5 million pixels)
- Active area coverage >65 %
- Single-photon sensitivity between 200-600 nm
- Magnetic fringe field <25 G
- Read-out:
  - Compatible with LHC 40MHz bunch crossing frequency
  - 10% occupancy (worst case)

Cms /HCAL read-out with HPDs

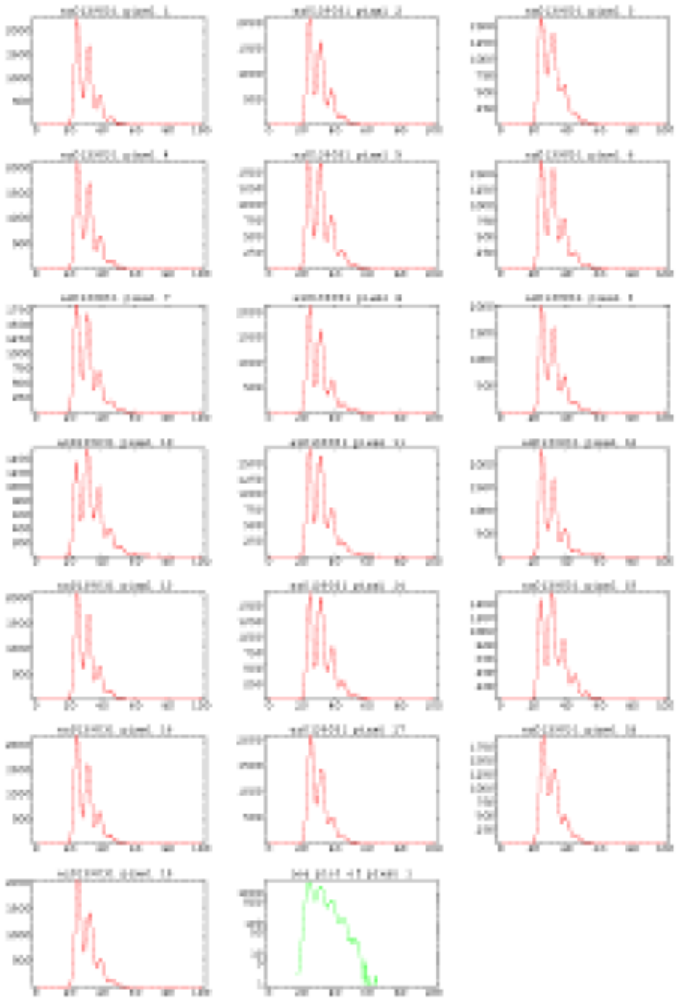

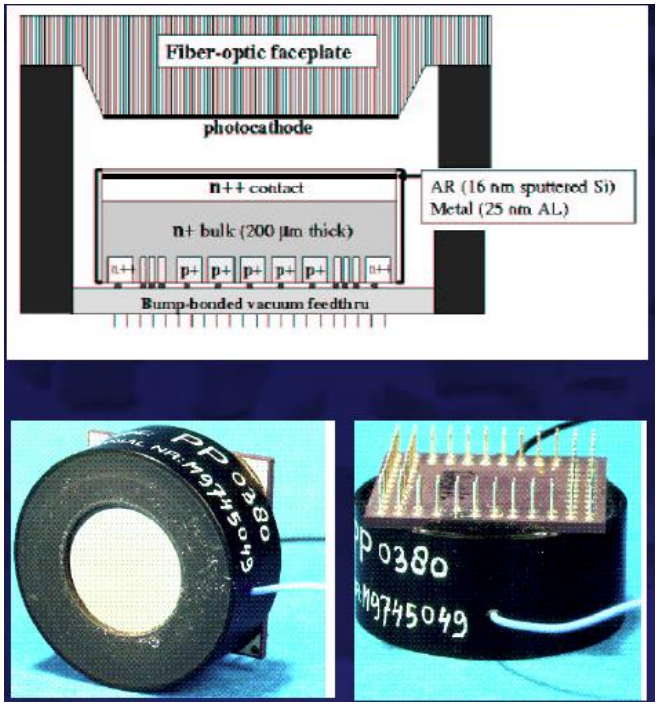

- Proximity focused optics.
- 27 mm active diameter
- S20 photocathode
- 19 or 73 hex pixels, 5.4 or 2.68 mm flat-to-flat
- Very small acceleration gap (3.3 mm)
- Gain = 2500 (12 kV)
- External electronics

Avalanche Photo Diode (APD) : an all-silicon device.

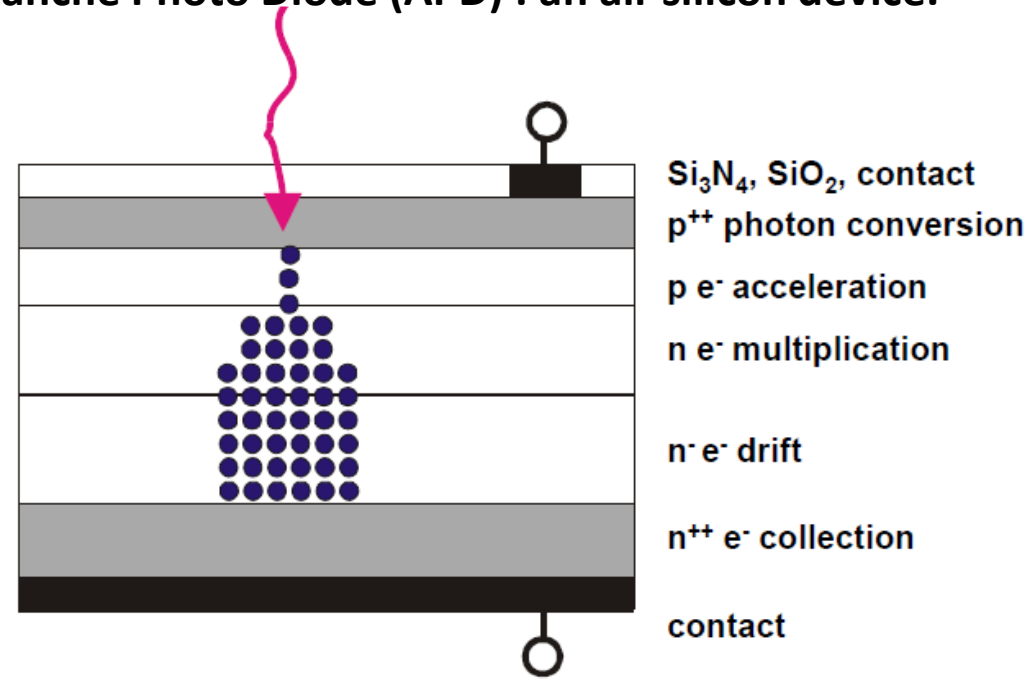

- high photo conversion
  $Q_{eff} \approx 0.7$
- Very high electric field
  10^5 V/m(avalanche mode)
- Thick
- Linear mode

Good tolerance with mag. Field
good (?) tolerance to radiation

Avalanche photodiodes have internal gain which improves the signal to noise ratio but still some 20 photons are needed for a detectable signal. The excess noise, the fluctuations of the avalanche multiplication limits the useful range of gain. CMS is the first big experiment that uses APD's.

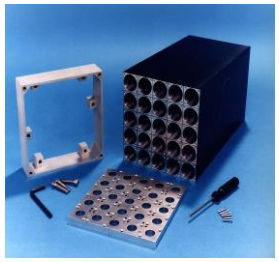

CMS APDs : ≈ 141 500 Pieces for the ECAL (scintillator : $PWBO_4$)

Active size : 5 x 5 mm^2

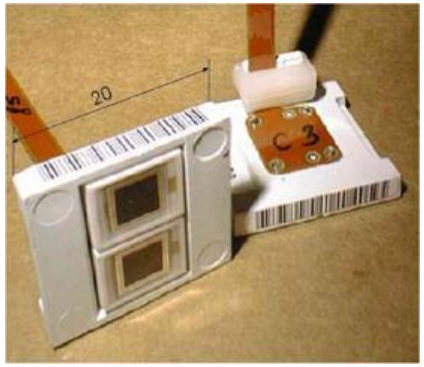

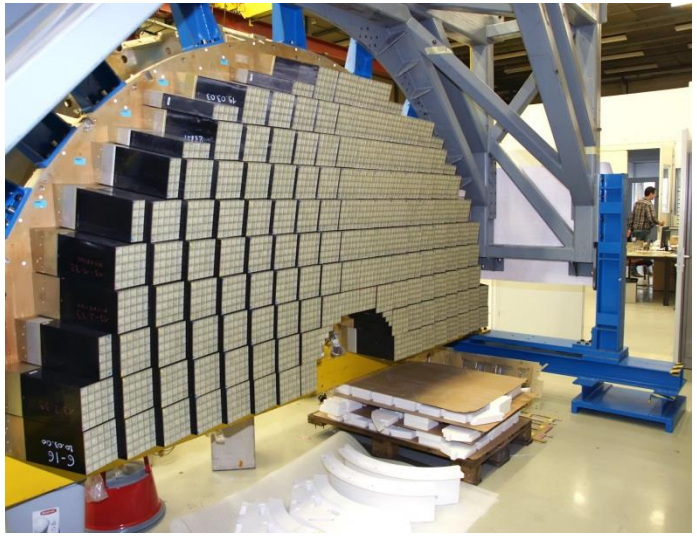

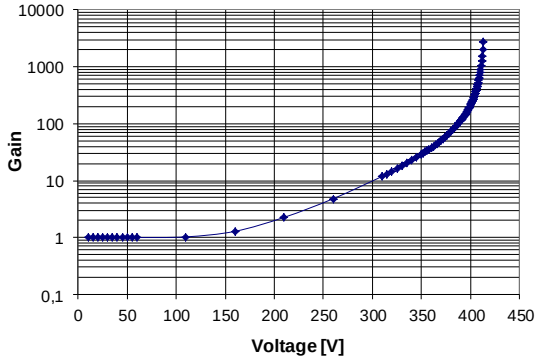

Jean-Marie Brom (IPHC) – brom@in2p3.fr

PPD : Pixelized Photon Detector = SiPM : Silicon Photomultplicator

= APDs in parallel with resistors

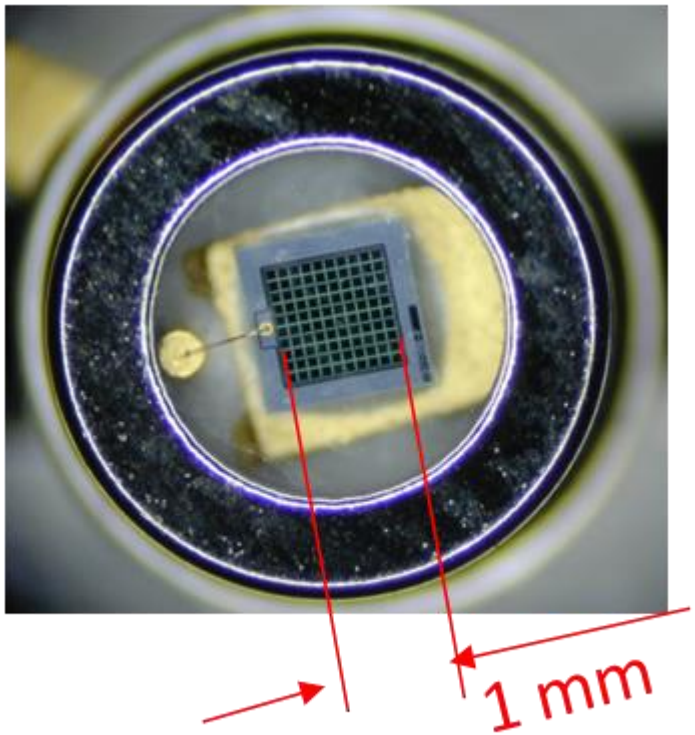

- high photo conversion
  $Q_{eff} \approx 0.7$
- Very high Gain (10^5)
- Geiger mode
- Pixellized
- Not a proportional counter
- Very good position counter
- Adapted to fibers (small surface)

SiPM's can detect single photons. They have been developed and described since the beginning of this millennium (patent of Z. Sadygov 1996).

Scintillation : SiPM

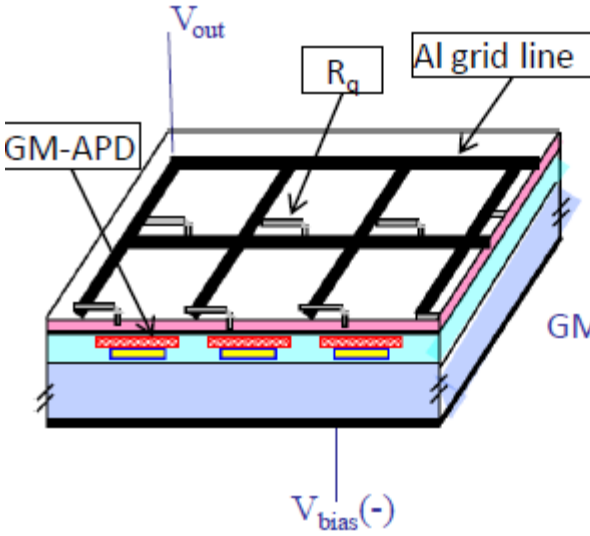

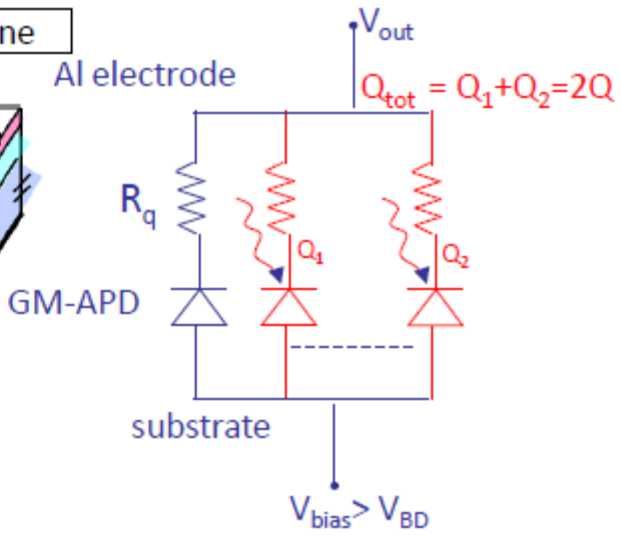

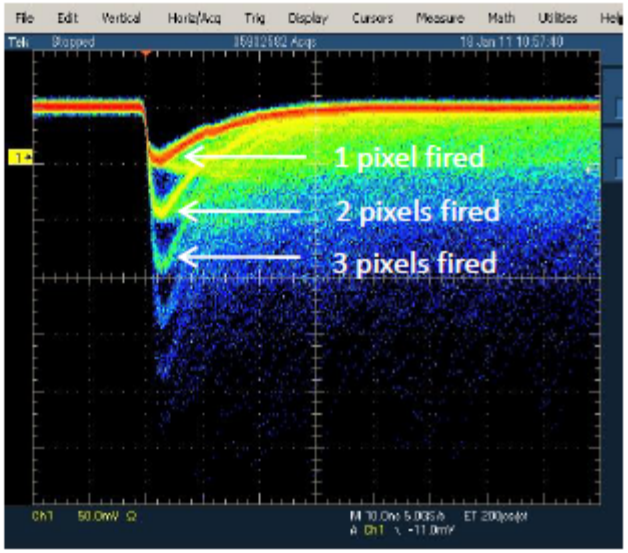

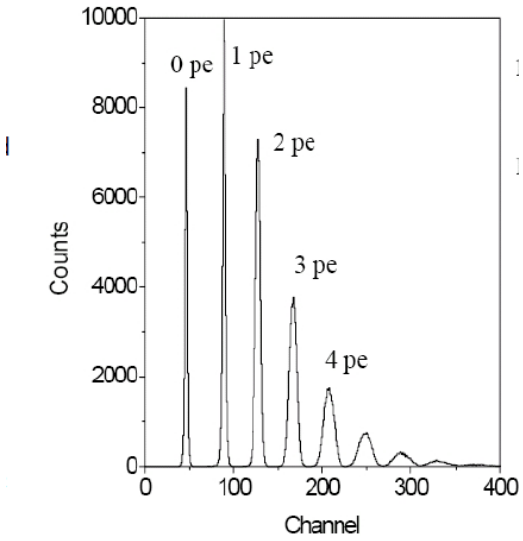

Advantages

- ☺ high gain (10^5-10^6) with low voltage (<80V)
- ☺ low power consumption (<75μW/mm²)
- ☺ fast (timing resolution ~ 50 ps RMS for single photons)
- ☺ insensitive to magnetic field (tested up to 7 T)
- ☺ high photon detection efficiency (30-40% blue-green)
- ☺ mechanically robust and compact

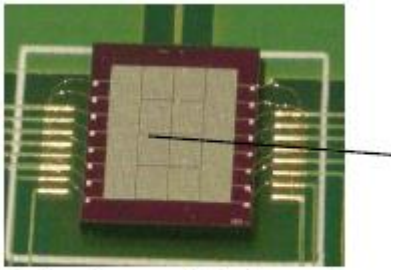

Each channel: 1x1 mm²
625 cells, 40x40 μm²/cell

Possible drawbacks

- ☹ high dark count rate (DCR)
  - early productions: ~100kHz – 1MHz/mm² at T~25°C; th=0.5pe
  - today productions: ~20kHz at T~25°C; th=0.5pe
  - thermal carriers, cross-talk, after-pulses
- ☹ temperature dependence
  - V_{BD}, signal shape, R_q, DCR , PDE

Scintillation : Photomultiplier

	PMT	APD	HPD	SiPM
Photon detection efficiency:				
blue	20%	50%	20%	12%
green - yellow	a few %	60-70%	a few %	15%
red	<1%	80%	<1%	15%
Gain	10^6-10^7	100-200	10^3	10^6
High voltage	1-2 kV	100-500 V	20 kV	25 V
Operation in the magnetic field	problematic	OK	OK	OK
Threshold sensitivity S/N≫1	1 ph.e.	~10 ph.e.	1 ph.e.	1 ph.e.
Timing /10 ph.e.	~100 ps	a few ns	~100 ps	30 ps
Dynamic range	$\sim 10^6$	large	large	$\sim 10^3/mm^2$
Complexity	high (vacuum, HV)	medium (low noise electronics)	very high (hybrid technology, very HV)	relatively low

	ATLAS	CMS
Magnetic field	2 T solenoid + toroid: 0.5 T (barrel), 1 T (endcap)	4 T solenoid + return yoke
Tracker	Silicon pixels and strips + transition radiation tracker $\sigma/p_T \approx 5 \cdot 10^{-4} p_T + 0.01$	Silicon pixels and strips (full silicon tracker) $\sigma/p_T \approx 1.5 \cdot 10^{-4} p_T + 0.005$
EM calorimeter	Liquid argon + Pb absorbers $\sigma/E \approx 10\%/\sqrt{E} + 0.007$	$PbWO_4$ crystals $\sigma/E \approx 3\%/\sqrt{E} + 0.003$
Hadronic calorimeter	Fe + scintillator / Cu+LAr (10λ) $\sigma/E \approx 50\%/\sqrt{E} + 0.03$ GeV	Brass + scintillator (7 λ + catcher) $\sigma/E \approx 100\%/\sqrt{E} + 0.05$ GeV
Muon	$\sigma/p_T \approx 2\%$ @ 50GeV to 10% @ 1TeV (Inner Tracker + muon system)	$\sigma/p_T \approx 1\%$ @ 50GeV to 10% @ 1TeV (Inner Tracker + muon system)
Trigger	L1 + HLT (L2+EF)	L1 + HLT (L2 + L3)

Čerenkov Detectors

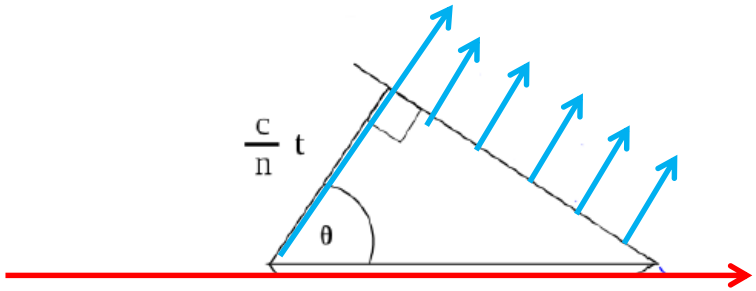

Particle travelling faster than light in a given medium emits radiation (photons)

$$\cos\theta_c = \frac{\frac{c}{nt}}{\beta ct} = \frac{1}{\beta n}$$

$$\cos\theta_c \leq 1 \longrightarrow \beta \geq \frac{1}{n} \quad N = 370L\int \varepsilon \sin^2\theta_c \, dE \quad \theta_c < \theta_{max}$$

$$\theta_{max} = cos^{-1}\left(\frac{1}{n}\right)$$

The emission of Čerenkov light depens directly from the speed of the particle
depens indirectly from the mass of the particle (p = m)
The maximum angle depens only from the medium.

Typical : 0.35 µm < $\lambda_{cerenkov}$ < 0.55 µm (usual medium : 1 < n < 2)

Radiation intensity (Franck-Tamm formula) : $$\frac{d^2N_{phot}}{dLd\lambda} = \frac{2\pi\alpha\, sin^2\theta}{\lambda^2}$$

α = 1 / 137
λ = Cerenkov light
θ = Cerenkov angle

in a wavelength interval 350-500 nm (photomultiplier tube), $\frac{dN}{dx} = 390 \sin^2\theta \; photons/cm$

Medium	n	Θ_{max}	$N_{photons}$
He	1.000035	0.48	0.39
Air	1.000283	1.36	3.12
Freon (gas)	1.00072	2.17	7.95
Isobutane	1.00127	2.89	14.91
Freon (liquid)	1.233	35.8	1899
Water	1.33	41.2	2407
Plexigas	1.5	48.2	3084

For a charged (1) particle, β = 1

Threshold Crenekov detectors make a simple decision on wether the particle is above or below the Cerenkov threshold velocity.

Used for differentiating heavy particles (π, K, p)

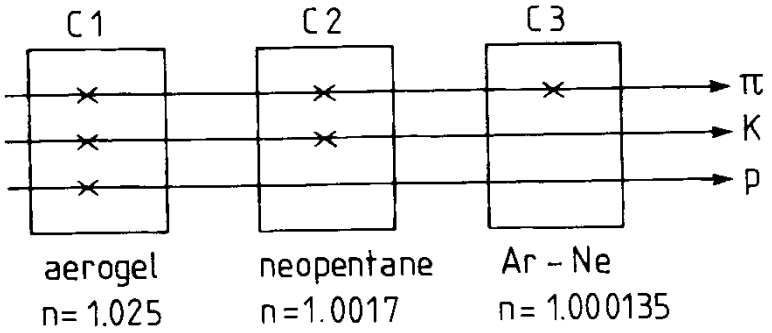

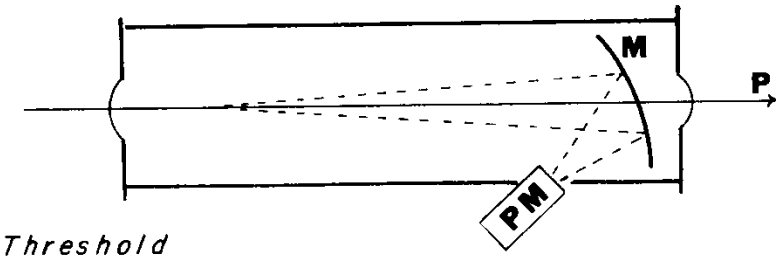

Changing the the gas pressure
Changes the refractive index

Aerogel : silicate gel (99.8% Air)

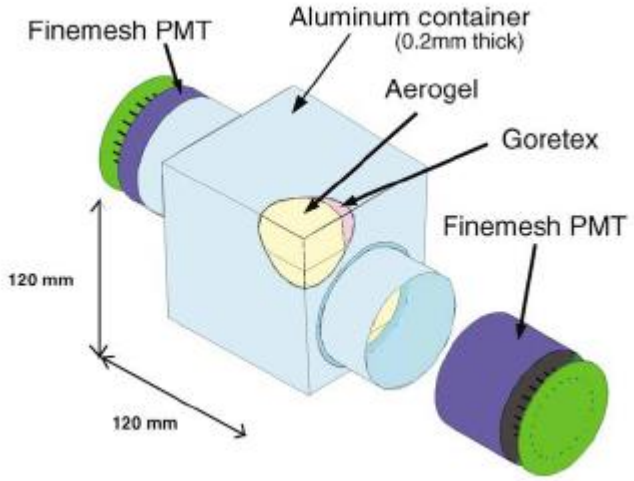

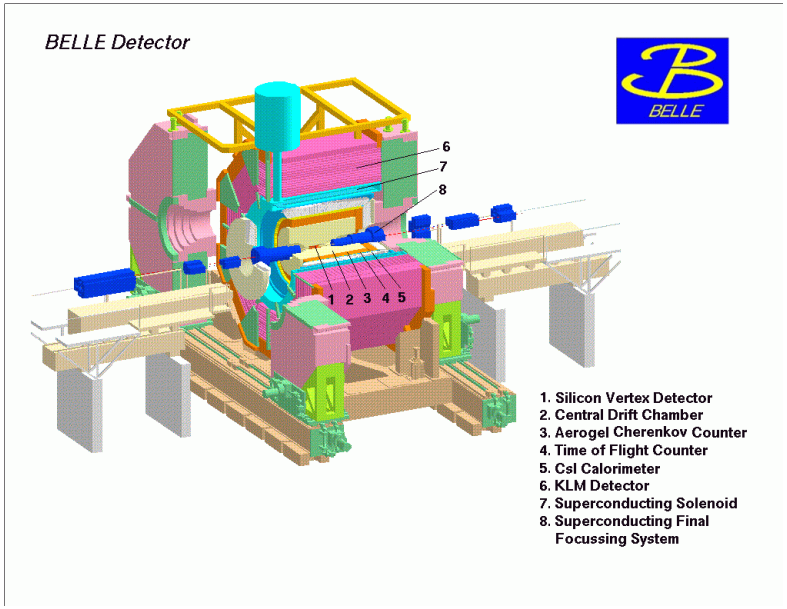

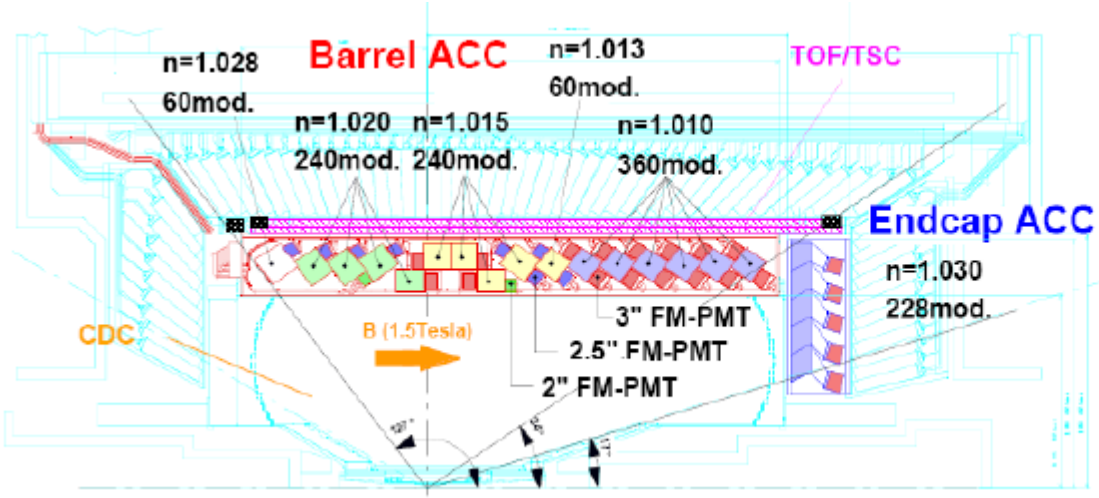

- Five aerogel tiles inside an aluminum box lined with a white reflector(Goretex reflector)
- Performance from test-beam

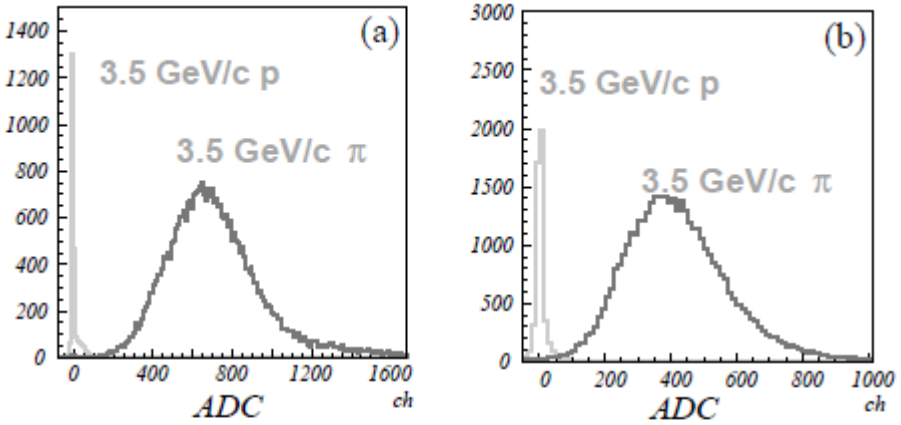

Fig. 47. Pulse-height spectra for 3.5 GeV/c pions (above threshold) and protons (below threshold) obtained by a single module of ACC in (a) non-magnetic field and (b) a magnetic field of 1.5 T. Silica aerogels with $n = 1.015$ were stacked to form the module.

Ring Imaging Cherenkov (Ypsilantis and Seguinot -1977)

- Measures both the Cherenkov angle and the number of photoelectrons detected.
- Can be used over particle identification over large surfaces.
- Requires photodetectors with single photon identification capability.

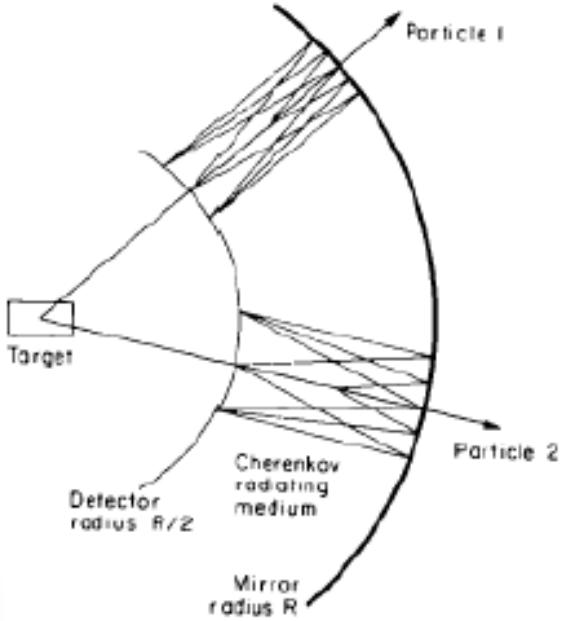

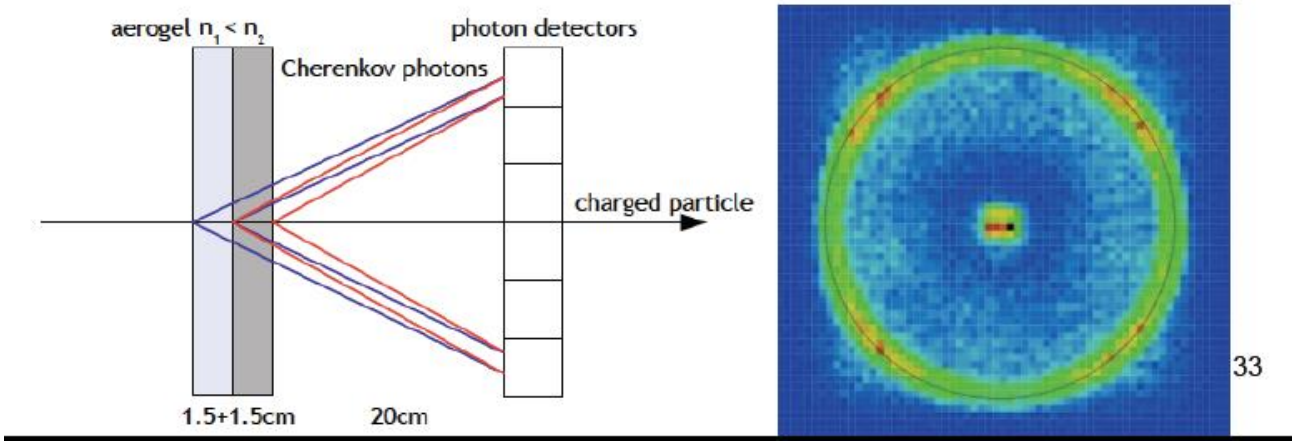

The LHCb RICH

C_4F_{10} in RICH 1 (n = 1.0014)
CF_4 in RICH 2 (n = 1.005)
Read-out : HPDs

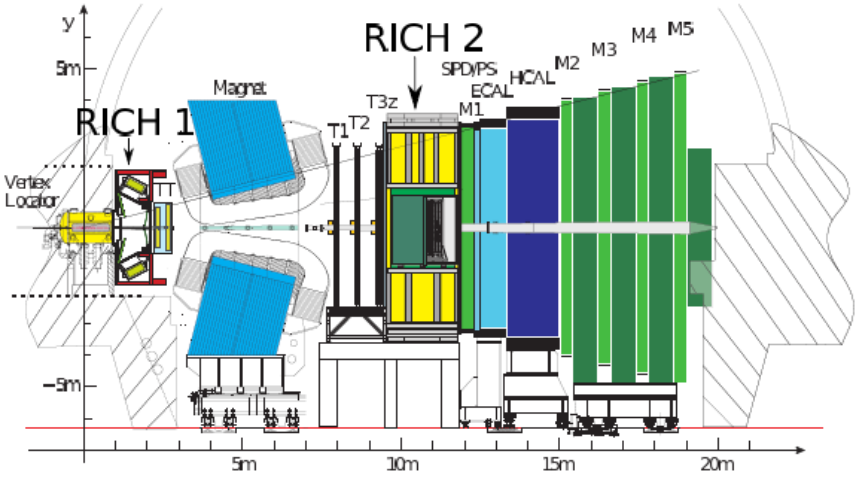

Figure 1: Side view of the LHCb spectrometer, with the two RICH detectors indicated

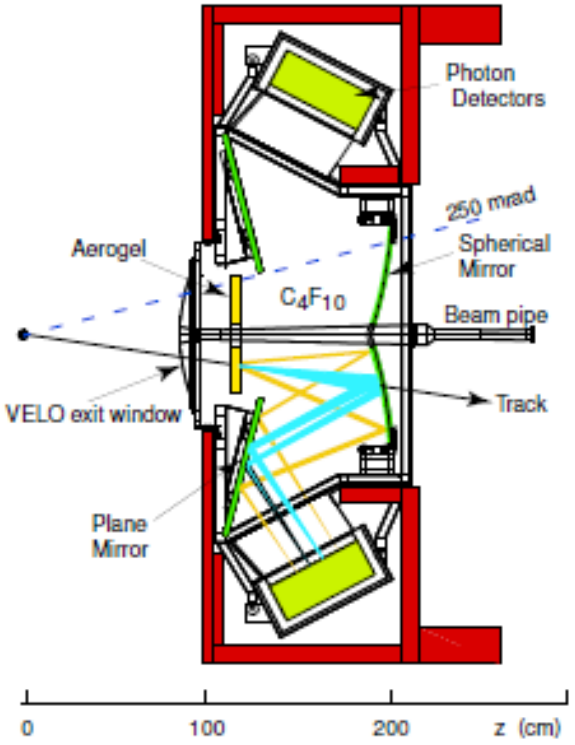

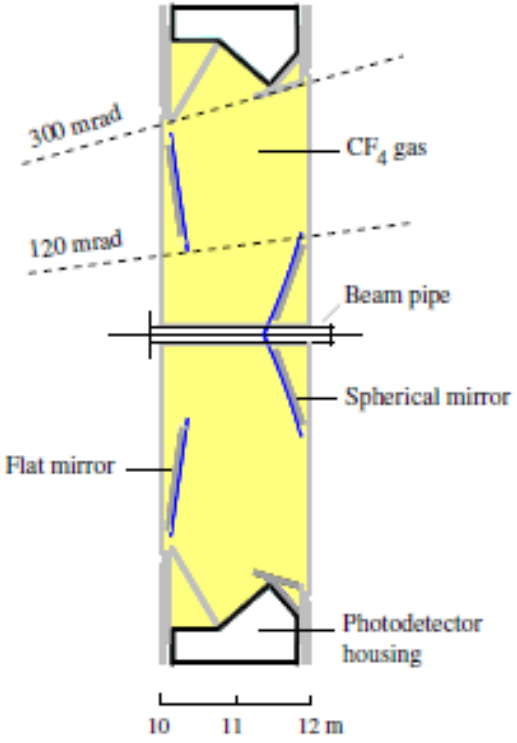

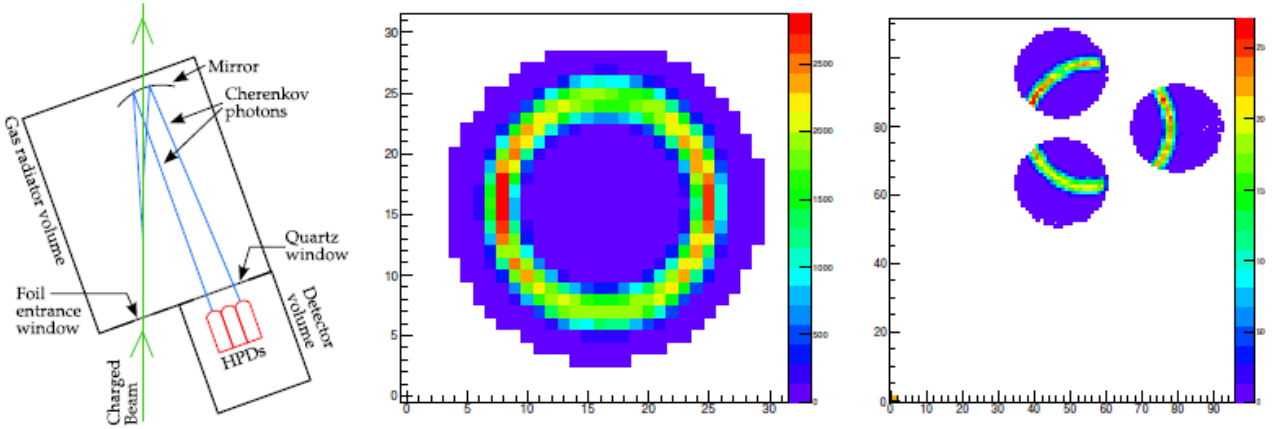

Figure 6: LEFT: *View from above of the arrangement of apparatus for the beam tests at Frascati and CERN. Electrons or charged pions enter the radiator, and produce Cherenkov photons in the Cherenkov radiator medium, which are reflected by the mirror and can then be detected by the HPDs.* CENTRE: *Display of Cherenkov ring in* N_2 *radiator, integrated over a run of ~38,500 events;* RIGHT: *Cherenkov ring in* C_4F_{10} *split across three HPDs (~35,000 events).*

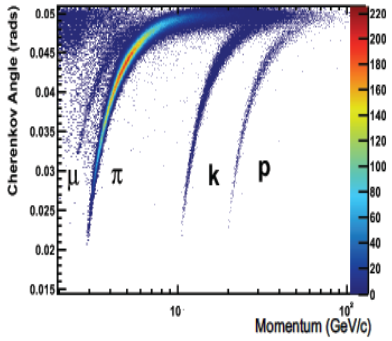

Figure 14: Reconstructed Cherenkov angle as a function of track momentum in the C_4F_{10} radiator

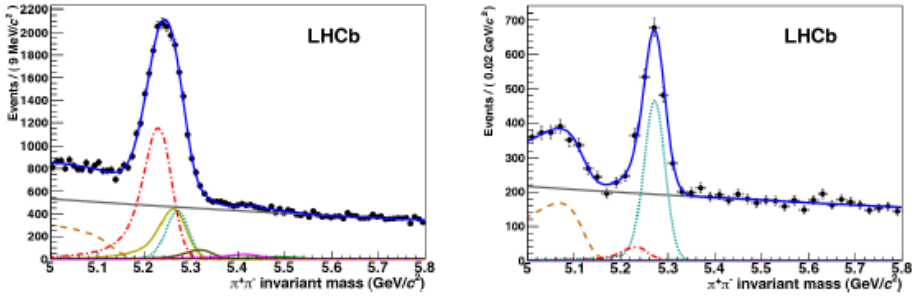

Figure 2: Invariant mass distribution for B→ h^+h^- decays [3] in the LHCb data before the use of the RICH information (left), and after applying RICH particle identification (right). The signal under study is the decay $B^0 \to \pi^+\pi^-$, represented by the turquoise dotted line. The contributions from different *b*-hadron decay modes ($B^0 \to K\pi$ red dashed-dotted line, B^0 →3-body orange dashed-dashed line, $B_s \to KK$ yellow line, $B_s \to K\pi$ brown line, $\Lambda_b \to pK$ purple line, $\Lambda_b \to p\pi$ green line), are eliminated by positive identification of pions, kaons and protons and only the signal and two background contributions remain visible in the plot on the right. The grey solid line is the combinatorial background

Transition radiation is a photon emission (X) occuring when a charged particle passes through inhomogeneous media, such as a boundary between two different media with different dielectric properties

Emission at an angle $\cos\theta = \frac{1}{\gamma}$

Very low rate ~ 1/2 α (fine structure constant)

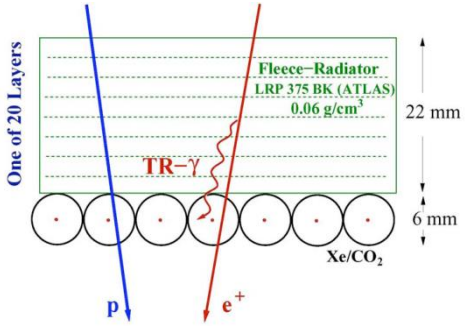

Transition Radiation Detector

ALICE TRD

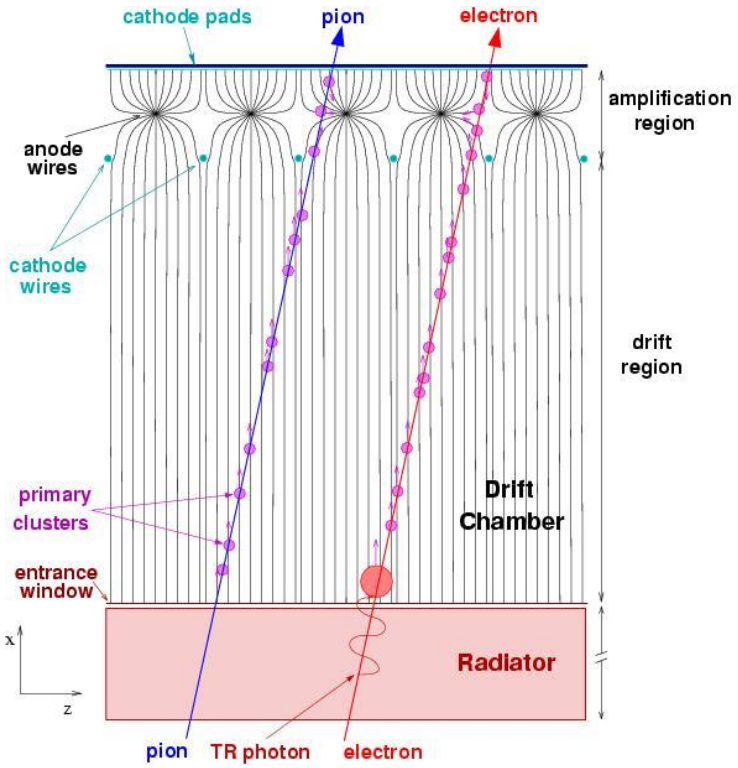

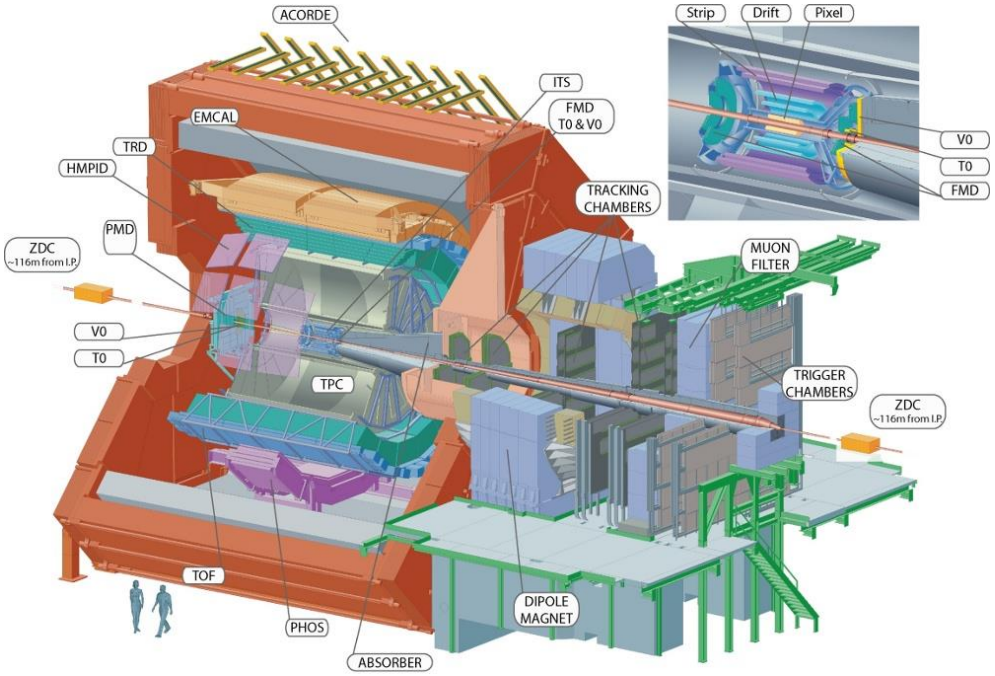

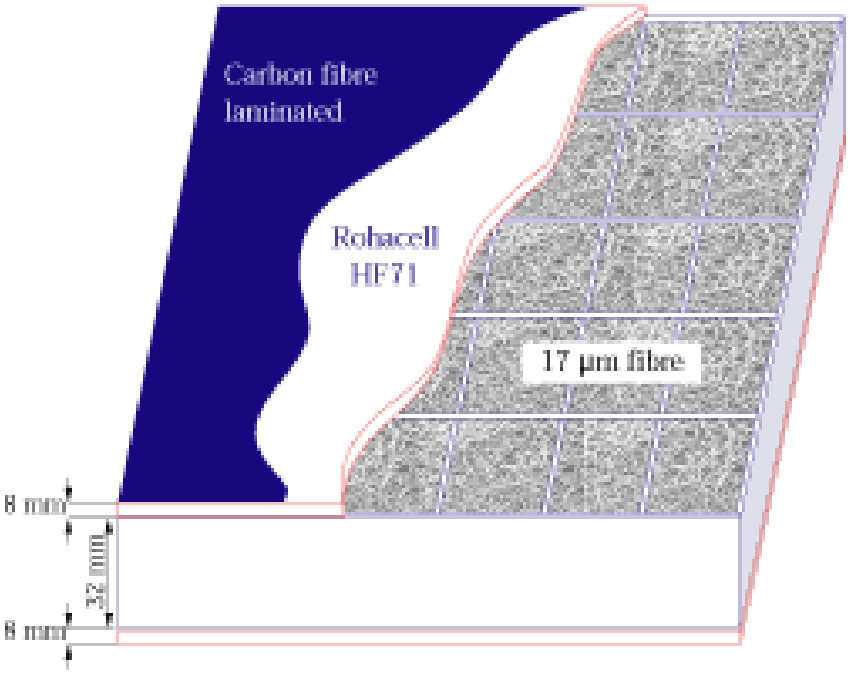

ALICE TRD

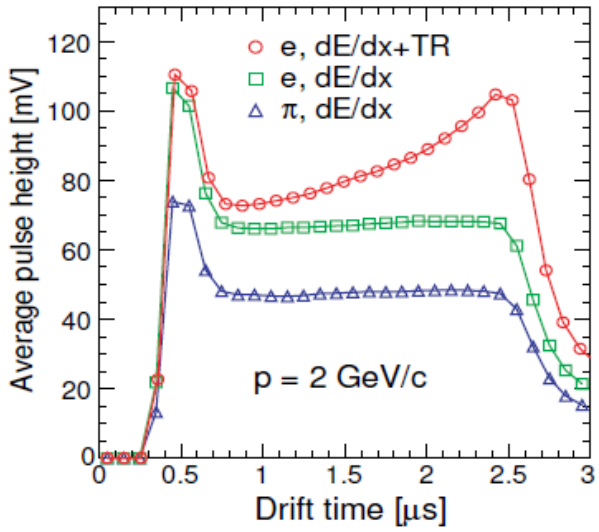

Figure 4: Average pulse height as function of the drift time.

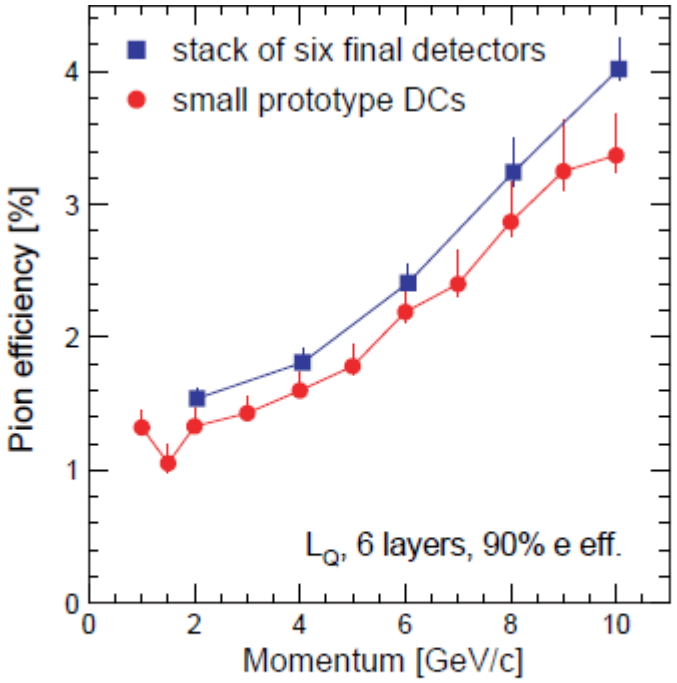

Figure 9: Measured electron identification performance.

ATLAS TRT : Combination Tracker / TRD

About 300 000 Straw tubes : position measurement by dE/dX
radiation occurs on the wall of the tube

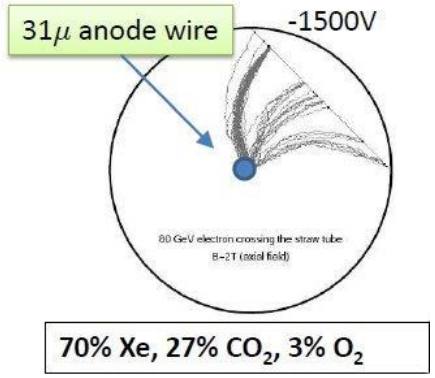

- Energy deposited in TRT, average event:
  - Sum of ionization losses of charged particles: ~2.5 keV
  - Deposition due to transition radiation photon absorption: >5 keV

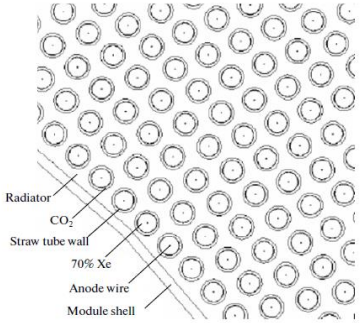

Fig. 5. Arrangement of straws in the module of the TRT

Table 1. Parameters of the barrel and end-cap modules

	$\|z\|_{min}$, mm	$\|z\|_{max}$, mm	R_{min}, mm	R_{max}, mm	Modules	Layers	Straws in a module
Barrel (both sides)	**0**	**780**	**554**	**1082**	**96**	**73**	**52 544**
Module of type 1 (inner)	400	712.1	563	624	32	9	329
Module of type 1 (outer)	7.5	712.1	625	694		10	
Module of type 2	7.5	712.1	697	860	32	24	520
Module of type 3	7.5	712.1	863	1066	32	30	793
End-cap modules (one side)	**827**	**2744**	**615**	**1106**	**20**	**160**	**122 880**
Module of type A	848	1705	644	1004	12	8	6144
Module of type B	1740	2710	644	1004	8	8	6144

ATLAS TRT : Combination Tracker / TRD

About 300 000 Straw tubes : position measurement by dE/dX
radiation occurs on the wall of the tube

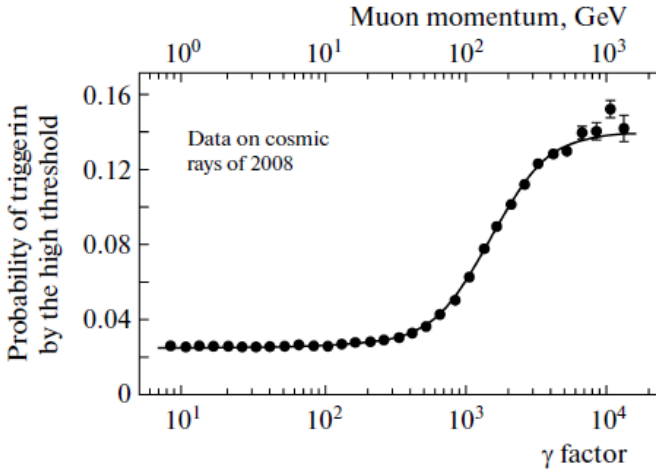

Fig. 14. Probability that a transition radiation photon will be produced in the ATLAS TRT vs. the Lorentz factor of the cosmic muon: the experimental data are shown with dots, and the fit is presented with a solid line.

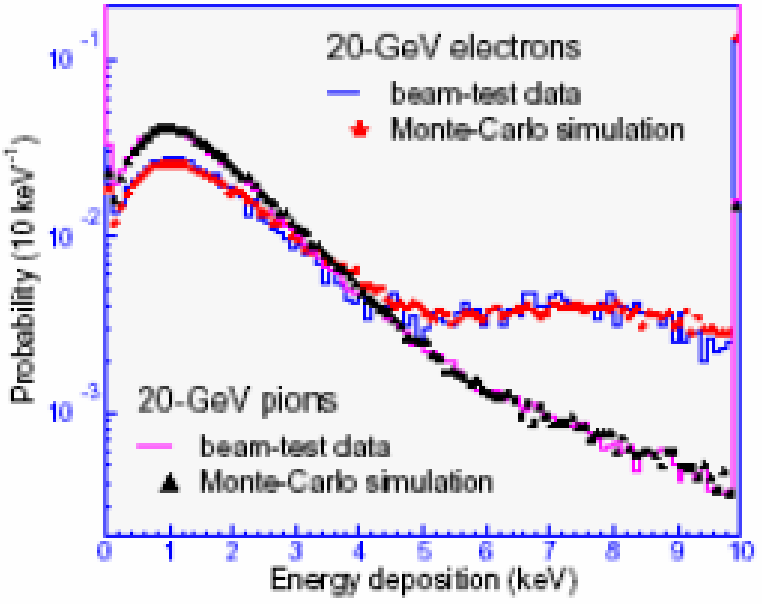

Differential energy spectra from data and simulation for a single straw with radiator


That's all Folks!